Enzymatic transformation of nonfood biomass to starch

Chun You[a,1], Hongge Chen[a,b,1], Suwan Myung[a,c], Noppadon Sathitsuksanoh[a,c], Hui Ma[d], Xiao-Zhou Zhang[a,d], Jianyong Li[e], and Y.-H. Percival Zhang[a,c,d,f,g,2]

[a]Biological Systems Engineering Department, [c]Institute for Critical Technology and Applied Science, and [e]Biochemistry Department, Virginia Polytechnic Institute and State University, Blacksburg, VA 24061; [b]College of Life Sciences, Henan Agricultural University, Zhengzhou 450002, China; [d]Gate Fuels, Inc., Blacksburg, VA 24060; [f]BioEnergy Science Center, Department of Energy, Oak Ridge, TN 37831; and [g]Cell Free Bioinnovations, Inc., Blacksburg, VA 24060

Edited* by Arnold L. Demain, Drew University, Madison, NJ, and approved March 27, 2013 (received for review February 5, 2013)

The global demand for food could double in another 40 y owing to growth in the population and food consumption per capita. To meet the world's future food and sustainability needs for biofuels and renewable materials, the production of starch-rich cereals and cellulose-rich bioenergy plants must grow substantially while minimizing agriculture's environmental footprint and conserving biodiversity. Here we demonstrate one-pot enzymatic conversion of pretreated biomass to starch through a nonnatural synthetic enzymatic pathway composed of endoglucanase, cellobiohydrolyase, cellobiose phosphorylase, and alpha-glucan phosphorylase originating from bacterial, fungal, and plant sources. A special polypeptide cap in potato alpha-glucan phosphorylase was essential to push a partially hydrolyzed intermediate of cellulose forward to the synthesis of amylose. Up to 30% of the anhydroglucose units in cellulose were converted to starch; the remaining cellulose was hydrolyzed to glucose suitable for ethanol production by yeast in the same bioreactor. Next-generation biorefineries based on simultaneous enzymatic biotransformation and microbial fermentation could address the food, biofuels, and environment trilemma.

bioeconomy | food and feed | synthetic amylose | in vitro synthetic biology | cell-free biomanufacturing

The continuing growth of the population and food consumption per capita means that the global demand for food could increase by 50–100% by 2050 (1, 2), and ∼30% of the world's agricultural land and 70% of the world's fresh water withdrawals are being used for the production of food and feed to support 7 billion people (3, 4). Starch is the most important dietary component because it accounts for more than half of the consumed carbohydrates, which provide 50–60% of the calories needed by humans. Starch is composed of polysaccharides consisting of a large number of glucose units joined together primarily by alpha-1,4-glycosidic bonds and alpha-1,6-glycosidic bonds. Linear-chain amylose is more valuable than branched amylopectin because it can be used as a precursor for making high-quality transparent, flexible, low-oxygen-diffusion plastic sheets and films (5, 6); tailored functional food or additives for lowering the risk of serious noninfectious diseases (e.g., diabetes and obesity) (7, 8); and a potential high-density hydrogen carrier (9–11). Also, it is easy to convert linear amylose to branched amylopectin by using alpha-glucan–branching glycosyltransferase (12).

Cellulose, a linear glucan linked by beta-1,4-glycosidic bonds, is the supporting material of plant cell walls and the most abundant carbohydrate on Earth. The annual resource of cellulosic materials is ∼40 times greater than the starch produced by crops cultivated for food and feed. In addition, (perennial) cellulosic plants and dedicated bioenergy crops can grow on low-quality land, even on marginal land, and require fewer inputs such as fertilizers, herbicides, pesticides, and water, whereas annual high-productivity starch-rich crops require high-quality arable land, enough water, and high inputs (4, 13). Every ton of cereals harvested is usually accompanied by the production of two to three tons of cellulose-rich crop residues, most of which are burned or wasted rather than used for cellulosic biorefineries (4, 14).

The cost-effective transformation of nonfood cellulose to starch could revolutionize agriculture and reshape the bioeconomy, while maintaining biodiversity, minimizing agriculture's environmental footprint, and conserving fresh water (4, 15). This transformation would not only promote the cultivation of plants chosen for rapid growth rather than those optimized for starch production, but it would also efficiently use marginal land for the production of the biomass required to meet the increasing needs for biofuels and renewable materials (4, 16–18). Some cellulolytic microorganisms can accumulate microbial glycogen, but maximum glycogen yields are very low, for example, 2–4% (wt/wt) (19, 20). These low yields are due mainly to the fact that the majority of the carbon source is used for the synthesis of cell mass rather than of glycogen (19, 20). Researchers in the field of synthetic biology wish to develop high-yield, glycogen-accumulating cellulolytic microorganisms, but this task remains challenging because of their complicated cellular systems (17).

The cost-effective release of soluble fermentative sugars from cellulosic materials through enzymatic hydrolysis is essential in second-generation cellulosic biorefineries (21). In enzymatic hydrolysis, a soluble hydrolytic intermediate, cellobiose, a major product of cellobiohydrolases (CBHs; EC 3.2.1.91), is rapidly hydrolyzed to glucose by adding excessive beta-glucosidase (BG) to prevent product inhibition of CBHs and endoglucanases (EGs; EC 3.2.1.4). Glucose cannot be used directly for the synthesis of starch because of the required energy input for the formation of alpha-1,4-glycosidic bonds among the glucose units. For example, in vivo starch and glycogen are usually synthesized from activated precursors such as ADP-glucose in plants and UDP-glucose in animals (22).

In vitro synthetic biology enables the rapid construction of nonnatural enzymatic pathways and often has more appealing advantages, such as higher product yields, faster reaction rates, and better tolerances to toxic compounds, than those mediated by living organisms (10, 23–31). Here we design a cell-free biosystem composed of a synthetic enzymatic pathway that can transform solid cellulose into amylose in high yields. This pathway is composed of several extracellular hydrolytic enzymes and two intracellular enzymes. These enzymes are separated by the cellular membrane in natural systems. A bioprocess called simultaneous enzymatic biotransformation and microbial fermentation (SEBF)

Author contributions: C.Y., H.C., and Y.-H.P.Z. designed research; C.Y. and H.C. performed research; S.M., H.M., and X.-Z.Z. contributed new reagents/analytic tools; C.Y., H.C., N.S., J.L., and Y.-H.P.Z. analyzed data; and H.C. and Y.-H.P.Z. wrote the paper.

Conflict of interest statement: The authors have filed a provisional patent disclosure (Zhang Y-HP, Chen H. Conversion of cellulose to starch through an in vitro synthetic enzymatic pathway. Filed on December 17, 2012.).

*This Direct Submission article had a prearranged editor.

[1]C.Y. and H.C. contributed equally to this work.

[2]To whom correspondence should be addressed. E-mail: ypzhang@vt.edu.

This article contains supporting information online at www.pnas.org/lookup/suppl/doi:10.1073/pnas.1302420110/-/DCSupplemental.

was developed to coproduce amylose, ethanol, and single-cell protein in one bioreactor to meet different needs from (tailored) food and feed to renewable materials and biofuels.

Results

We designed an enzymatic pathway that can transform cellulose to amylose (Fig. 1*A*). This pathway has two modules: (*i*) partial hydrolysis of cellulose to cellobiose by optimizing the CBH and EG composition and ratio and (*ii*) amylose synthesis using a glycoside hydrolase family 9 cellobiose phosphorylase (CBP; EC 2.4.1.20) and a glycosyltransferase family 35 alpha-glucan phosphorylase (αGP; EC 2.4.1.1). In this system, CBP reversibly converts cellobiose to glucose-1-phosphate (G-1-P) and glucose in the presence of phosphate ions, the special αGP adds one glucose unit from G-1-P at the nonreducing end of amylose or maltodextrins, and phosphate ions are recycled to maintain nearly constant pH and phosphate levels (Fig. 1*A*).

Five cellulase components were used to optimize the cellulose degradation and hydrolysis product distribution of the pretreated Avicel regenerated amorphous cellulose (RAC). These cellulases included two EGs, glycoside hydrolase family 5 *Bacillus subtilis* endoglucanase (BsCel5) and *Trichoderma* spp. endoglucanase II (TrCel5A), and three CBHs, family 7 *Trichoderma* spp. cellobiohydrolase (TrCel7A), family 9 *Clostridium phytofermentans* cellobiohydrolase (CpCel9), and family 48 *C. phytofermentans* cellobiohydrolase (CpCel48) (32). All recombinant enzymes were produced in *Escherichia coli* BL21 (DE3) and purified to homogeneity (Fig. S1*A*), except for the *Trichoderma* enzymes, which were purchased. The sole cellulase component did not efficiently hydrolyze pretreated cellulose, whereas combinations of an EG and a CBH led to higher cellulose degradation (Table S1). However, the distribution of soluble products from glucose to cellotriose varied greatly, depending on the enzyme combination (Fig. S1*B* and Table S2). Based on the cellobiose yield and the cellulose degradation (Fig. S1*C* and Table S1), the best cellulase combination was bacterial BsCel5 and fungal TrCel7A.

A combination of the *Clostridium thermocellum* CBP (33, 34) and the special αGP was used for the synthesis of amylose from cellobiose. Although building blocks for in vitro synthetic biology projects are highly interchangeable (28), we found that whether amylose was synthesized from cellobiose depended on the choice of αGP. Three αGPs, one from potato (*Solanum tuberosum*) and two thermophilic bacteria, *C. thermocellum* (35) and *Thermotoga maritima*, were tested. Among them, only the potato αPG (PGP) was able to drive the reversible reactions mediated by CBP and αGP toward the synthesis of amylose.

The one-pot transformation of RAC to amylose was implemented by four enzymes, BsCel5, TrCel5A, CBP, and PGP, in 0.5 mL of reaction volume (Fig. 1*B*). The RAC slurry (Fig. 1*B*, tube 1) was completely hydrolyzed and then converted into amylose (tube 3). The synthetic amylose exhibited a deep blue color in the presence of iodine (tube 4), whereas the negative control (cellulose/iodine) was yellow (tube 2). The soluble amylose was precipitated by the addition of ethanol (tube 5). The amylose yield was 14.4% (wt/wt) (i.e., 0.144 g of amylose per gram of cellulose), and the number-average degree of polymerization was ~150. The addition of glucose oxidase to remove glucose, a strong inhibitor of CBP, resulted in a yield increase to 30.0% (wt/wt) (tube 6) (Fig. S2). However, the use of glucose oxidase resulted in a net loss in glucose (36). The number-average of degree of polymerization varied from 140 to 250, depending on the amount of maltotetraose added and cellobiose availability

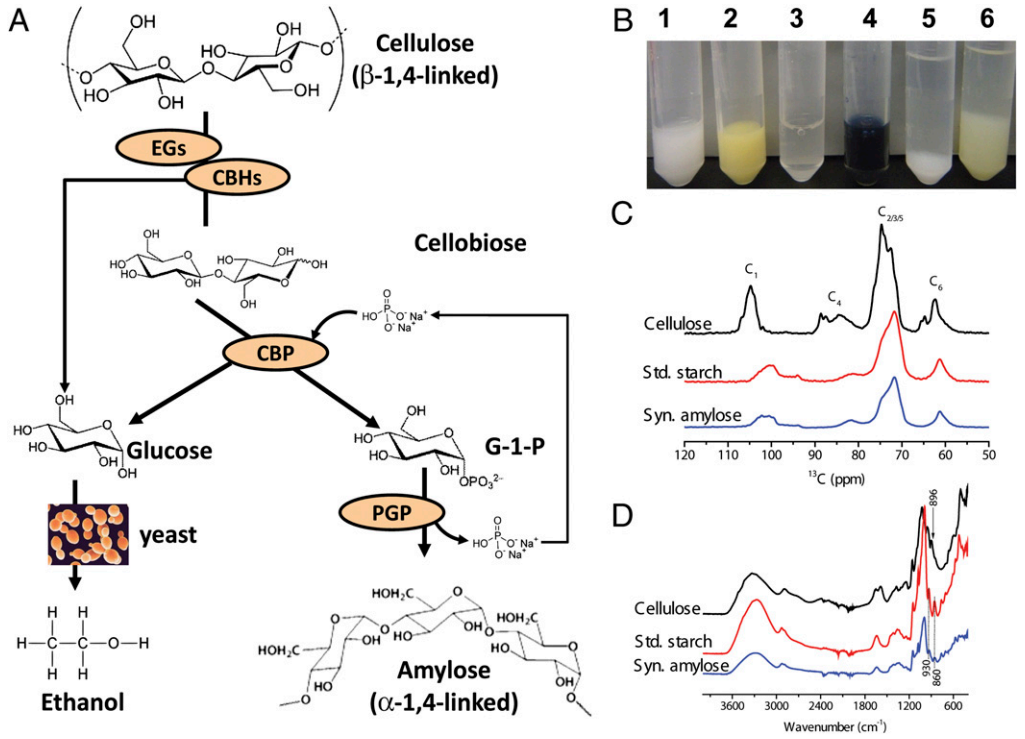

Fig. 1. The enzymatic cellulose hydrolysis using endoglucanases (EGs), cellobiohydrolases (CBHs) and beta-glucosidase (BG) in cellulosic ethanol biorefinery versus the synthetic cellulose-to-amylose pathway supplemented with cellobiose phosphorylase (CBP) and potato alpha-glucan phosphorylase (PGP) (*A*). Characterization of synthetic starch by iodine dyeing (*B*), CP/MAS ^{13}C-NMR (*C*), and FTIR (*D*). Tube 1, cellulose-suspended solution; tube 2, cellulose solution plus iodine/potassium iodide; tube 3, water-soluble synthetic starch solution made from cellulose mediated by the four- enzyme mixture; tube 4, synthetic starch solution plus iodine/potassium iodide; tube 5: precipitated starch by ethanol addition; and tube 6, precipitated starch when the mixture was supplemented with glucose oxidase.

(Table S3), where maltotetraose was used as the primer for amylose synthesis catalyzed by PGP. Synthetic amylose was validated by the hydrolysis of glucoamylase, followed by a hexokinase-based glucose assay, cross-polarization magic-angle spinning ^{13}C-NMR (Fig. 1*C*), and FTIR (Fig. 1*D*). Cellulose exhibited completely different C1 and C4 peaks compared with the amylose standard and synthetic amylose (Fig. 1*C*). In the FTIR (Fig. 1*D*), the bands at 930 and 860 cm^{-1} are typical signatures of alpha-1,4–linked amylose. The band at 896 cm^{-1}, a signature of beta-1,4–linked cellulose, was not observed in the starch samples. The above evidence suggests that amylose was synthesized from cellulose.

Among the three tested αGP proteins, only PGP can synthesize amylose from cellobiose. A Basic Local Alignment Search Tool search of the PGP sequence against protein databases of various model species from bacteria to humans identified the related proteins. Comparison of these sequences indicated that the residues involved in substrate binding and catalysis were fairly conserved among all αGP sequences. Phylogenetic analysis suggests that these αGP enzymes evolved from a common ancestor, and the enzymes from the original plant were evolutionally conserved (Fig. 2). The *C. thermocellum* αGP and the *T. maritima* αGP were highly similar to each other but were far different from PGP. We built homology structure models for all αGPs and observed that PGP and four other plant αGPs (*Ipomoea batatas*, *Spinacia oleracea*, *Oryza sativa*, and *Triticum aestivum*) had a special cap on their catalytic site that was absent in all bacterial αGPs and other plant αGPs (e.g., *Zea mays* and *Arabidopsis thaliana*). Fig. 3*A* illustrates the major structural difference between PGP and *T. maritima* αGP. Therefore, we hypothesized that the polypeptide cap on the catalytic site of PGP was responsible for driving low-concentration G-1-P toward the synthesis of amylose. We designed two PGP mutants; one had a part of the polypeptide cap removed and the other did not have the cap at all (Fig. S3 and Tables S4 and S5). In the buffer containing cellobiose and CBP, the partially decapped PGP (PDC-PGP) had decreased amylose synthesis ability compared with wildtype (Fig. 3*B*, tube 2), whereas the completely decapped PGP (CDC-PGP) lost this ability completely (Fig. 3*B*, tube 3). The K_m and k_{cat} values of PGP, PDC-PGP, CDC-PGP, and *C. thermocellum* αGP are compared in Table 1. The removal of the cap of PGP decreased the k_{cat}/K_m values from 3.33 to 0.43 mM^{-1}·s^{-1} in the starch synthesis direction and from 0.55 to 0.06 mM^{-1}·s^{-1} in the starch degradation direction. Compared with the *C. thermocellum* αGP, PGP has a higher k_{cat}/K_m value in the synthesis direction and a lower k_{cat}/K_m in the degradation direction, suggesting that wild-type PGP has a preferred function for starch synthesis to degradation. Additionally, PGP has a lower activation energy for synthesis and a high activation energy for degradation. This result suggests the importance of identifying the correct building blocks for in vitro synthetic biology systems.

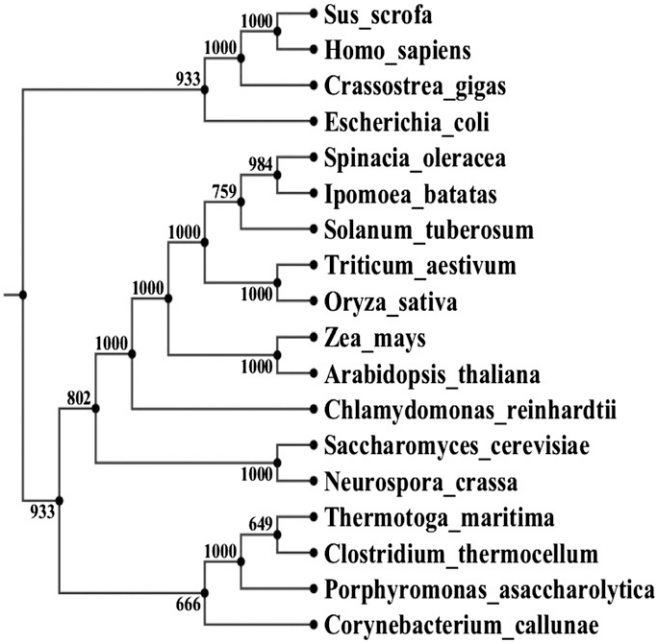

Fig. 2. A phylogenetic tree for the selected alpha-glucan phosphorylases.

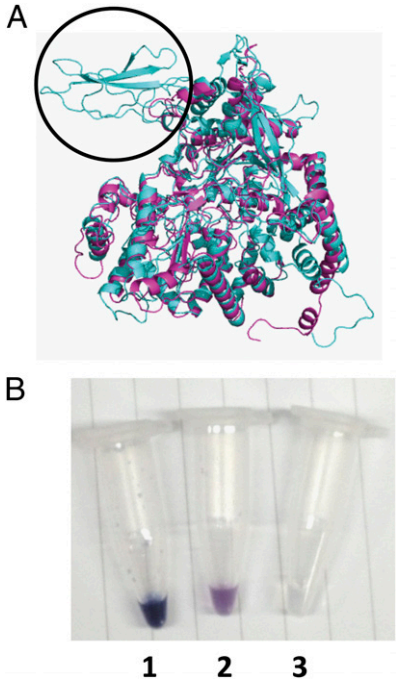

Fig. 3. Homology structure comparison between PGP (cyan) and *Thermotoga maritima* alpha-glucan phosphorylase (purple) (*A*) and photos of starch-synthesizing ability (*B*) from cellobiose mediated by CBP and wild-type PGP (tube 1), partially decapped PGP (tube 2), or completely decapped PGP (tube 3).

To achieve selective recycling of CBP and PGP from the enzymatic cellulose hydrolysate and fermentation broth, we also developed a simple enzyme purification and coimmobilization process using Avicel-containing nanomagnetic particles (A-NMPs) (Fig. 4). A-NMPs with a diameter of 400–600 nm were synthesized (Fig. 4*A*) according to the modified solvothermal synthesis method (37). Family 3 cellulose-binding module (CBM3)–containing proteins (e.g., CBM3-containing green fluorescent protein) can be bound tightly on the surface of A-NMPs because of the high-affinity adsorption of CBM3 on the surface of cellulose. The immobilized CBM3-containing enzyme or complex on A-NMPs can be easily separated from the aqueous solution using a magnetic field (Fig. 4*B*). We produced three recombinant proteins in *E. coli* BL21 (DE3): miniscaffoldin (38), CtDoc-LL-PGP, and CBP-RfDoc (Tables S4 and S5). The synthetic protein miniscaffoldin contained one CBM3, one cohesin module from CipA of *C. thermocellum*, one cohesin module from CbpA of *Clostridium cellulovorans*, and one cohesin module of ScaB from *Ruminococcus flavefaciens* in tandem (38). CtDoc-LL-PGP was composed of a *C. thermocellum* dockerin and PGP linked by a long linker. CBP-RfDoc was composed of *C. thermocellum* CBP and a *R. flavefaciens* dockerin. Because of the high-affinity interaction among cohesins and dockerins, the three proteins can be self-assembled as an enzyme complex (Fig. 4*C*). Therefore, we prepared the immobilized CBP–PGP complex on A-NMPs by mixing three cell extracts with

Table 1. Comparison of potato alpha-glucan phosphorylase and mutants and a thermophilic *C. thermocellum* alpha-glucan phosphorylase

Name	Amylose synthesis*				Amylose degradation†				k_{cat}/K_m ratio, syn/deg¶	E_a ratio, syn/deg¶
	k_{cat}, s^{-1}	K_m,‡ mM	k_{cat}/K_m, $mM^{-1}\cdot s^{-1}$	E_a,§ KJ/moL	k_{cat}, s^{-1}	K_m,‡ mM	k_{cat}/K_m, $mM^{-1}\cdot s^{-1}$	E_a,§ KJ/moL		
PGP	5.83 ± 0.34	1.76 ± 0.18	3.33	18.3	0.90 ± 0.11	1.64 ± 0.13	0.55	59.7	6.5	0.31
PDC-PGP	4.88 ± 0.27	1.92 ± 0.21	2.54	14.4	0.83 ± 0.09	2.20 ± 0.21	0.38	26.6	5.9	0.54
CDC-PGP	0.95 ± 0.11	2.22 ± 0.41	0.43	13.4	0.19 ± 0.04	3.11 ± 0.23	0.06	20.7	5.0	0.65
CthαGP	6.6 ± 0.3	1.9 ± 0.2	3.50	50.6	8.1 ± 0.2	0.39 ± 0.01	21.0	16.8	0.8	3.01

*The activities were assayed at 37 °C in a 100 mM Hepes buffer (pH 7.4) containing 10 mM Mg^{2+}, 20 mM G1P at maltodextrin (419672; Sigma; dextrose equivalent of 4.0–7.0) concentrations between 0.2 and 5 times their respective K_m values.
†The activities were assayed at 37 °C in a 100 mM Hepes buffer (pH 7.4) containing 10 mM Mg^{2+} and 20 mM inorganic phosphate at various maltodextrin concentrations between 0.2 and 5 times their respective K_m values.
‡The concentrations of maltodextrin were given as the molar concentration of the nonreducing ends.
§The Arrhenius plot was depicted as $\ln(k_{cat})$ versus 1/T (K) and the activation energy (E_a) was calculated from the slope of the plot.
¶Syn/deg means synthesis/degradation.

A-NMPs followed by magnetic separation (Figs. S4 and S5). The immobilized CBP–PGP enzyme complexes exhibited the same reaction rates as the noncomplexed CBP and PGP mixture (Fig. 4*D*), suggesting that this enzyme coimmobilization did not impair enzymatic activity.

We developed a bioprocess, SEBF, that can transform pretreated biomass to amylose, ethanol, and yeast as single-cell protein in one bioreactor (Fig. 1*A*). This process may be regarded as modified simultaneous saccharification and fermentation (SSF) in second-generation cellulosic biorefineries, where beta-glucosidase was replaced with immobilized CBP–PGP that can be easily recycled by a magnetic force. In the proof-of-concept SEBF experiment, we used a mixture of fungal TrCel7A, bacterial BsCel5, and CpCel48 (32) for hydrolyzing pretreated biomass, such as RAC, and diluted acid (DA)-pretreated and cellulose solvent- and organic solvent-based lignocellulose fractionation (COSLIF)-pretreated corn stover (39). In this system, nonused glucose units generated from the cellulases and CBP were assimilated by ethanol-producing

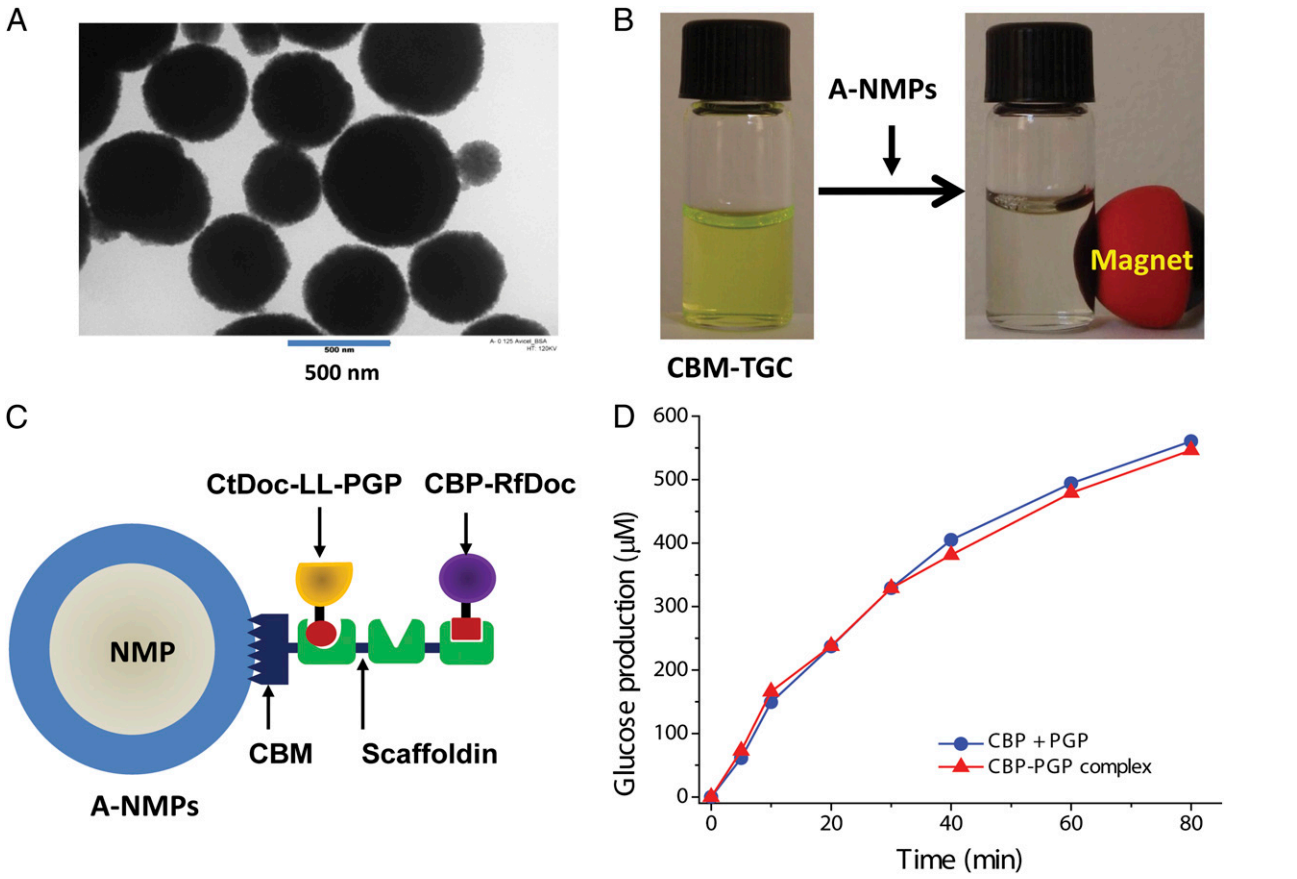

Fig. 4. Transmission electron microscopic image of Avicel-containing nanomagnetic particles (A-NMPs) (*A*), photos of A-NMPs that bind with a CBM3-tagged green fluorescent protein under magnet (*B*), the scheme of coimmobilized PGP and CBP on the A-NMPs (*C*), and starch synthesis rate comparison based on glucose formation between the coimmobilized PGP–CBP and the noncomplexed PGP and CBP mixture (*D*).

Saccharomyces cerevisiae; the yeast can produce ethanol and single-cell proteins because the yeast cannot use cellobiose and G-1-P (40, 41); a mixture of 75 μM maltodextrins with a dextrose equivalent of 16.5–19.5 was used for the primer for amylose synthesis. Under the applied conditions, the amylose yields were 25%, 23%, and 2% for RAC, COLISF-pretreated corn stover, and DA-pretreated corn stover at hour 12, respectively (Table 2). A lower cellulose digestion yield was obtained for DA-pretreated biomass because the homemade enzyme mixtures were optimized for efficient hydrolysis of amorphous cellulose rather than of crystalline cellulose and hemicellulose- and lignin-containing biomass. We also tested two commercial fungal enzyme mixtures, gifted by Novozymes and Genencor, for the hydrolysis of pretreated biomass. Much higher cellulose hydrolysis yields were obtained but ample beta-glucosidase in the commercial cellulase mixtures rapidly converted cellobiose to glucose, resulting in very low yields of amylose. After SEBF, immobilized CBP–PGP can be recycled and ethanol can be separated by distillation; the precipitated synthetic amylose is extracted using 1 M NaOH and precipitated by neutralization for obtaining high-quality amylose. The yeast cells and the biomass residuals remained in solid pellets.

Discussion

This cellulose-to-amylose biotransformation could be scaled up by increasing the stability of CBP and PGP and decreasing their production costs in terms of cost per kilogram of enzyme (Fig. S6), because this combined cellulose-hydrolyzing and starch-synthesizing enzyme mixture did not involve any labile coenzymes [e.g., CoA and NAD(P)] (Fig. 1*A*); no glucose released from the cellulose was wasted (Fig. 1); only two more enzymes were added, and they can be reused easily by a magnetic force (Fig. 4); and no energy or costly reagents were added. When both CBP–PGP enzymes have total turnover number (TTN) values of 2.6×10^6 mol of product per mole of enzyme and their cost is 20 US dollars per kilogram of enzyme, the extra enzyme cost compared with SSF in biorefineries would be 1 cent per kilogram of amylose synthesized. When enzyme costs are lower than \$20/kg and/or TTN values are higher than 2.6×10^6, the enzyme expenditure could be decreased drastically (Fig. S6). Wild-type thermophilic CBP has an estimated TTN value of $\sim 2 \times 10^6$ at 30 °C (34), whereas more stable engineered CBP by combining directed evolution and rational design has an enhanced TTN value of $\sim 2 \times 10^7$, by a factor of ~10 (42). Wild-type PGP has an estimated TTN value of $\sim 6 \times 10^4$ at 30 °C. Via directed evolution, a PGP mutant has a nearly two orders of magnitude enhancement in TTN values, being $\sim 1.7 \times 10^6$ (43). By considering the stability of immobilized glucose isomerase (29) and other immobilized thermophilic enzymes (44), further stability improvement of CBP and PGP is expected to be achieved by more rounds of mutagenesis plus enzyme immobilization soon. Another scale-up challenge could be low-cost production of CBP and PGP. Considering the production costs of bulk enzymes such as cellulase and protease (~\$10/kg) (45) and relatively fine enzymes used for biocatalysis (~\$100/kg) (30, 46), the above economic analysis based on enzyme stability and enzyme production costs could be feasible after more research and development efforts. In partial support of this, enzyme costs in the enzymatic hydrolysis of starch are only 0.3–0.6 cents per kilogram of starch hydrolyzed (29).

The theoretical yield of amylose from cellulose through this synthetic pathway is 50%, higher than the yields that we currently obtained. The practical amylose yield could be enhanced through more cellobiose production by optimizing the cellulase mixture composition and ratio, eliminating beta-glucosidase from the commercial cellulase mixtures, optimization of CBP–PGP loading, improving PGP performance, process design (47), and biomass pretreatment conditions. For potential application, the current amylose yields (e.g., 2–30%) in biorefineries would be acceptable because no sugar is wasted and the potential market for synthetic starch as food and feed could be less than 1/10th that of biofuels and biochemicals (4, 48).

Synthetic amylose has a variety of applications from high-value to low-value products, depending on its quality and potential market sizes. Top-quality amylose can be used as a chromatographic column matrix and drug capsule material in the pharmaceutical industry. Amylose can be used to make biodegradable plastics; starch-based plastics already account for 50% of the bioplastic market (5). High-quality amylose is suitable for producing transparent and flexible low-oxygen-diffusion plastic sheets and films (6). Amylose is an important thickener, water binder, emulsion stabilizer, and gelling agent in the food industry. Food-grade amylose can be blended with cereals and processed to high-amylose tailored foods for meeting special dietary needs because high-amylose wheat, corn, and rice have a much lower glycemic load. The foods with lower glycemic loads can improve human health and lower the risk of serious noninfectious diseases (e.g., diabetes and obesity) (7, 8). Medium-quality amylose can be used as a high-density hydrogen carrier for the enzymatic production of starchy hydrogen, which could solve the challenges associated with hydrogen production, hydrogen storage, infrastructure, and safety concerns (9–11). After SEBF, low-quality amylose that is mixed with yeast cells after centrifugation can be used directly as animal feed for nonruminant animals, such as pigs and chickens, for which yeast cells are currently a supplementary protein source.

To meet the growing needs for biofuels and renewable materials, as well as food and feed, whose production requires large amounts of arable land, water, and energy, there is an urgent need to use abundant and renewable nonfood agricultural and forest residues and dedicated bioenergy crops that can grow on marginal land and require low inputs. Future biorefineries based on this technology could help address the food, biofuels, and environment trilemma; decrease the impact of growing food and feed consumption on the environment; provide more healthy food; and promote the bioeconomy. Because in vitro building blocks cannot duplicate themselves, the large-scale implementation of cellulose-to-starch in future biorefineries would not raise the questions about ethics, biosecurity, and biosafety that are often confronted by in vivo synthetic biology projects.

Materials and Methods

Chemicals and Materials. Cellobiohydrolase I (TrCel7A) and endoglucanase II (TrCel5A) from *Trichoderma* spp. were purchased from Megazyme. All other enzymes expressed in *E. coli* were purified and concentrated as described elsewhere and in *SI Materials and Methods*. Insoluble regenerated amorphous cellulose (RAC) was prepared from Avicel PH105 (FMC) using concentrated phosphoric acid. Corn stover was obtained from the National

Table 2. The yields of synthetic amylose from various types of pretreated biomass at hour 12

Biomass type	Solid concentration, g/L	Cellulose content, %	Cellulose degraded, %	Amylose produced, g/L	Amylose yield, % (wt/wt)
RAC	20	100	77.2	3.82	24.7
COSLIF corn stover	38	45.7	49.4	1.97	23.0
DA corn stover	80	53.7	14.7	0.13	2.1

Reported values are the averages of three measurements, where the SDs were less than 10%.

Renewable Energy Laboratory. Experimental conditions for dilute sulfuric acid pretreatment and COSLIF were described previously (39).

Simultaneous Enzymatic Biotransformation and Fermentation. Simultaneous enzymatic biotransformation and fermentation was conducted under the following conditions: 100 mM Hepes buffer (pH 7.3) containing 20 g/L RAC, 38 g/L COSLIF-pretreated corn stover or 80 g/L DA-pretreated corn stover, 0.2 mg/mL BsCel5, 0.1 mg/mL CpCel48, 0.4 mg/mL commercial TrCel7A, 0.2 mg/mL A-NMPs immobilized CtCBP–PGP enzyme complex, 10 mM phosphate, 75 μM maltodextrin with a dextrose equivalent of 16.5–19.5, and yeast cells (final OD 0.5). Pretreated biomass was washed with water three times before use. Yeast cells were washed three times with PBS buffer (24 g/L NaCl, 0.6 g/L KCl, 5.4 g/L $Na_2HPO_4{\cdot}2H_2O$, and 0.84 g/L KH_2PO_4) before mixing them with other components. The reactions were carried out at 30 °C. The samples were taken at hour 12. The reactions were terminated by 5-min water boiling. After centrifugation, which removed denatured and precipitated enzymes, the supernatants were mixed with an equal volume of 100% ethanol to precipitate the synthetic starch. The precipitated starch was washed once with ethanol. The number of glucose units in the starch was measured by the phenol-sulfuric acid assay and enzymatic starch kit.

ACKNOWLEDGMENTS. This work was supported by the Biological Systems Engineering Department of Virginia Polytechnic Institute and State University and partially supported by the College of Agriculture and Life Sciences Biodesign and Bioprocessing Research Center, Shell GameChanger Program, and the Department of Energy BioEnergy Science Center (Y.-H.P.Z.). H.C. was partially supported by the China Scholarship Council.

1. Foley JA, et al. (2011) Solutions for a cultivated planet. *Nature* 478(7369):337–342.
2. Godfray HCJ, et al. (2010) Food security: The challenge of feeding 9 billion people. *Science* 327(5967):812–818.
3. The World Economic Forum Water Initiative (2011) *Water Security: The Water-Food-Energy-Climate Nexus* (Island Press, Washington, DC).
4. Zhang Y-HP (2013) Next-generation biorefineries will solve the food, biofuels and environmental trilemma in the energy-food-water nexus. *Energy Sci Eng*, 10.1002/ese3.2.
5. van Soest JJG, Vliegenthart JFG (1997) Crystallinity in starch plastics: consequences for material properties. *Trends Biotechnol* 15(6):208–213.
6. Frische R, Wollmann K, Gross-Lannert R, Schneider J, Best B (1994) US Patent 5374304. Special amyloses and their use for producing biodegradable plastics.
7. Regina A, et al. (2006) High-amylose wheat generated by RNA interference improves indices of large-bowel health in rats. *Proc Natl Acad Sci USA* 103(10):3546–3551.
8. Maki KC, et al. (2012) Resistant starch from high-amylose maize increases insulin sensitivity in overweight and obese men. *J Nutr* 142(4):717–723.
9. Zhang Y-HP, Huang W-D (2012) Constructing the electricity-carbohydrate-hydrogen cycle for a sustainability revolution. *Trends Biotechnol* 30(6):301–306.
10. Zhang Y-HP, Evans BR, Mielenz JR, Hopkins RC, Adams MWW (2007) High-yield hydrogen production from starch and water by a synthetic enzymatic pathway. *PLoS ONE* 2(5):e456.
11. Zhang Y-HP (2009) A sweet out-of-the-box solution to the hydrogen economy: Is the sugar-powered car science fiction? *Energy Environ. Sci.* 2(2):272–282.
12. Peat S, Bourne EJ, Barker SA (1948) Enzymic conversion of amylose into amylopectin. *Nature* 161(4082):127–128.
13. Lynd LR, Woods J (2011) Perspective: A new hope for Africa. *Nature* 474(7352): S20–S21.
14. Tuck CO, Pérez E, Horváth IT, Sheldon RA, Poliakoff M (2012) Valorization of biomass: Deriving more value from waste. *Science* 337(6095):695–699.
15. Somerville C, Youngs H, Taylor C, Davis SC, Long SP (2010) Feedstocks for lignocellulosic biofuels. *Science* 329(5993):790–792.
16. Sheppard AW, Gillespie I, Hirsch M, Begley C (2011) Biosecurity and sustainability within the growing global bioeconomy. *Curr. Opin. Environ. Sustain.* 3(1–2):4–10.
17. French CE (2009) Synthetic biology and biomass conversion: A match made in heaven? *J R Soc Interface* 6(Suppl 4):S547–S558.
18. Casillas CE, Kammen DM (2010) Environment and development. The energy-poverty-climate nexus. *Science* 330(6008):1181–1182.
19. Desvaux M, Guedon E, Petitdemange H (2001) Carbon flux distribution and kinetics of cellulose fermentation in steady-state continuous cultures of *Clostridium cellulolyticum* on a chemically defined medium. *J Bacteriol* 183(1):119–130.
20. Matheron C, Delort A-M, Gaudet G, Forano E, Liptaj T (1998) ^{13}C and ^{1}H nuclear magnetic resonance study of glycogen futile cycling in strains of the genus *Fibrobacter*. *Appl Environ Microbiol* 64(1):74–81.
21. Lynd LR, et al. (2008) How biotech can transform biofuels. *Nat Biotechnol* 26(2): 169–172.
22. Berg JM, Tymoczko JL, Stryer L (2002) *Biochemistry* (Freeman, New York), 5th Ed.
23. Wang Y, Huang W, Sathitsuksanoh N, Zhu Z, Zhang Y-HP (2011) Biohydrogenation from biomass sugar mediated by *in vitro* synthetic enzymatic pathways. *Chem Biol* 18(3):372–380.
24. Xu Y, et al. (2011) Chemoenzymatic synthesis of homogeneous ultralow molecular weight heparins. *Science* 334(6055):498–501.
25. Bujara M, Schümperli M, Pellaux R, Heinemann M, Panke S (2011) Optimization of a blueprint for *in vitro* glycolysis by metabolic real-time analysis. *Nat Chem Biol* 7(5): 271–277.
26. Swartz JR (2011) Transforming biochemical engineering with cell-free biology. *AIChE J* 58(1):5–13.
27. Guterl J-K, et al. (2012) Cell-free metabolic engineering: Production of chemicals by minimized reaction cascades. *ChemSusChem* 5(11):2165–2172.
28. Zhang Y-HP, Sun J-B, Zhong J-J (2010) Biofuel production by in vitro synthetic enzymatic pathway biotransformation. *Curr Opin Biotechnol* 21(5):663–669.
29. Zhang Y-HP (2010) Production of biocommodities and bioelectricity by cell-free synthetic enzymatic pathway biotransformations: Challenges and opportunities. *Biotechnol Bioeng* 105(4):663–677.
30. You C, Zhang Y-HP (2013) Cell-free biosystems for biomanufacturing. *Adv Biochem Eng Biotechnol* 131:89–119.
31. del Campo JSM, et al. (2013) High-yield dihydrogen production from xylose through cell-free synthetic cascade enzymes. *Angew Chem Int Ed Engl*, 10.1002/anie.201300766.
32. You C, Zhang X-Z, Sathitsuksanoh N, Lynd LR, Zhang Y-HP (2012) Enhanced microbial utilization of recalcitrant cellulose by an ex vivo cellulosome-microbe complex. *Appl Environ Microbiol* 78(5):1437–1444.
33. Ye X, et al. (2009) Spontaneous high-yield production of hydrogen from cellulosic materials and water catalyzed by enzyme cocktails. *ChemSusChem* 2(2):149–152.
34. Tanaka K, Kawaguchi T, Imada Y, Ooi T, Arai M (1995) Purification and properties of cellobiose phosphorylase from *Clostridium thermocellum*. *J Ferment Bioeng* 79(3): 212–216.
35. Ye X, Rollin J, Zhang Y-HP (2010) Thermophilic α-glucan phosphorylase from *Clostridium thermocellum*: Cloning, Characterization and Enhanced thermostability. *J Mol Catal, B Enzym* 65:110–116.
36. Ohdan K, Fujii K, Yanase M, Takaha T, Kuriki T (2007) Phosphorylase coupling as a tool to convert cellobiose into amylose. *J Biotechnol* 127(3):496–502.
37. Deng H, et al. (2005) Monodisperse magnetic single-crystal ferrite microspheres. *Angew Chem Int Ed Engl* 117(18):2842–2845.
38. You C, Myung S, Zhang Y-HP (2012) Facilitated substrate channeling in a self-assembled trifunctional enzyme complex. *Angew Chem Int Ed Engl* 51(35):8787–8790.
39. Rollin JA, Zhu Z, Sathitsuksanoh N, Zhang Y-HP (2011) Increasing cellulose accessibility is more important than removing lignin: A comparison of cellulose solvent-based lignocellulose fractionation and soaking in aqueous ammonia. *Biotechnol Bioeng* 108(1):22–30.
40. De Winter K, Cerdobbel A, Soetaert W, Desmet T (2011) Operational stability of immobilized sucrose phosphorylase: Continuous production of α-glucose-1-phosphate at elevated temperatures. *Process Biochem* 46(10):2074–2078.
41. Galazka JM, et al. (2010) Cellodextrin transport in yeast for improved biofuel production. *Science* 330(6000):84–86.
42. Ye X, Zhang C, Zhang Y-HP (2012) Engineering a large protein by combined rational and random approaches: Stabilizing the *Clostridium thermocellum* cellobiose phosphorylase. *Mol Biosyst* 8(6):1815–1823.
43. Yanase M, Takata H, Fujii K, Takaha T, Kuriki T (2005) Cumulative effect of amino acid replacements results in enhanced thermostability of potato type L α-glucan phosphorylase. *Appl Environ Microbiol* 71(9):5433–5439.
44. Myung S, Zhang X-Z, Percival Zhang YH (2011) Ultra-stable phosphoglucose isomerase through immobilization of cellulose-binding module-tagged thermophilic enzyme on low-cost high-capacity cellulosic adsorbent. *Biotechnol Prog* 27:969–975.
45. Klein-Marcuschamer D, Oleskowicz-Popiel P, Simmons BA, Blanch HW (2012) The challenge of enzyme cost in the production of lignocellulosic biofuels. *Biotechnol Bioeng* 109(4):1083–1087.
46. Tufvesson P, Lima-Ramos J, Nordblad M, Woodley JM (2011) Guidelines and cost analysis for catalyst production in biocatalytic processes. *Org Process Res Dev* 15(1): 266–274.
47. Vanderghem C, Boquel P, Blecker C, Paquot M (2010) A multistage process to enhance cellobiose production from cellulosic materials. *Appl Biochem Biotechnol* 160(8): 2300–2307.
48. MacKay DJC (2009) *Sustainable Energy–Without the Hot Air* (UIT Cambridge, Cambridge, UK).

Supporting Information

You et al. 10.1073/pnas.1302420110

SI Materials and Methods

Chemicals and Materials. All chemicals were reagent-grade or higher and purchased from Sigma-Aldrich or Fisher Scientific, unless otherwise noted. The PCR enzyme was Phusion DNA polymerase from New England BioLabs. The oligonucleotides were synthesized by Integrated DNA Technologies. Bacterial cellulase components were purified and concentrated as described previously (1, 2): glycoside hydrolase family 5 *Bacillus subtilis* endoglucanase (BsCel5) and family 48 *Clostridium phytofermentans* cellobiohydrolase (CpCel48). Insoluble regenerated amorphous cellulose (RAC) was prepared from Avicel PH105 (FMC) (3, 4). Water-soluble cellodextrin standards were prepared in mixed concentrated acids (5). Corn stover was obtained from the National Renewable Energy Laboratory. Corn was grown from biomass AgriProducts. Experimental conditions for dilute sulfuric acid pretreatment and cellulose solvent and organic solvent lignocellulose fractionation (COSLIF) were described previously (6).

Strains and Medium. *Escherichia coli* Top10 was used as a host cell for DNA manipulation, and *E. coli* BL21 Star (DE3) (Invitrogen) was used as a host cell for recombinant protein expression. LB medium was used for *E. coli* cell culture and recombinant protein expression. The final concentrations of antibiotics for *E. coli* were 100 mg/L ampicillin and 50 mg/L kanamycin. *Saccharomyces cerevisiae* S288c, a gift from Hong Lvu, Fudan University, Shanghai, China, was used to remove glucose in the cellulose-to-starch experiment.

Plasmid Construction. Plasmid pET20b-miniscaf had an expression cassette containing one family 3 cellulose-binding module (CBM3) and one cohesin module (314–723 aa) from CipA (GenBank accession no. L08665) of *Clostridium thermocellum* ATCC 27405, one cohesin module (1,078–1,253 aa) from CbpA (GenBank accession no. AAA23218.1) of *Clostridium cellulovorans* ATCC 35296, and one cohesin domain (28–186 aa) of ScaB (GenBank accession no. CAC34385.1) from *Ruminococcus flavefaciens* in tandem. The DNA sequence encoding this chimeric miniscaffoldin contained one CBM3 was synthesized by GenScript. The DNA sequence encoding this chimeric miniscaffoldin was amplified by PCR using a pair of primers (IF-scaf and IR-scaf); the pET20b vector backbone was amplified with a pair of primers (VF-scaf and VR-scaf). The two DNA templates were in vitro assembled to DNA multimers by prolonged overlap extension PCR (7). Five microliters of the PCR product containing 1 μg of DNA multimers was transformed to *E. coli* Top 10, yielding plasmid pET20b-miniscaf (8).

The full-length cDNA encoding potato alpha-glucan phosphorylase gene from *Solanum tuberosum* (*pgp*, GenBank accession no. D00520.1) was synthesized by GenScript. The *pgp* gene was amplified with a pair of primers [IF-potato alpha-glucan phosphorylase (PGP) and IR-PGP], the pET20b vector backbone was amplified with a pair of primers (VF-PGP and VR-PGP), and plasmid pET20b-*pgp* was obtained based on two DNA fragments by using simple cloning. For the easy purification the PGP using a synthetic scaffoldin (8), a dockerin (CtDoc, 699–741 aa) from *Clostridium thermocellum* Cel48S was engineered to add at the N terminal of PGP. The DNA sequence encoding CtDoc was amplified with a pair of primers (IF-CtDoc and VR-LL-PGP). A long linker (LL, 463–561 aa) from CipA of *C. thermocellum* was engineered between the CtDoc and PGP. The DNA sequence encoding LL was amplified with a pair of primers (IF-LL-PGP and IR-LL-PGP) from plasmid of pET20b-Mini-CipA (9). The pET20b vector backbone containing *pgp* was amplified with a pair of primers (VF-LL-PGP and VR-CtDoc) from pET20b-*pgp*. This plasmid pET20b-ctdoc-ll-pgp was constructed based on three DNA fragments by simple cloning (7).

Based on the homology modeling structure of PGP, a large cap exists inside this protein. To investigate the function of this cap, the plasmids with partially decapped and completely decapped pgp (pET20b-ctdoc-ll-pdc-pgp and pET20b-ctdoc-ll-cdc-pgp) were constructed based on the plasmid pET20b-ctdoc-ll-pgp using a Phusion site-directed mutagenesis kit (NEB). The primers for construction of pET20b-ctdoc-ll-pdc-pgp were PGP_PDC-F and PGP_PDC-R. The primers for construction of pET20b-ctdoc-ll-cdc-pgp were PGP_CDC-F and PGP_CDC-R. In short, the target linear plasmid was amplified with two phosphorylated primers, then the linear plasmid was recircularized by ligation with T4 ligase, then the circularized plasmid was transformed into *E. coli*, yielding pET20b-ctdoc-ll-pdc-pgp and pET20b-ctdoc-ll-cdc-pgp.

Plasmid pET20b-ctcbp had an expression cassette containing cellobiose phosphorylase (CtCBP; GenBank accession no. AAL67138.1) from *C. thermocellum*. The gene of CtCBP was amplified from the genomic DNA of *C. thermocellum* and then subcloned into pET20b, yielding pET20b-ctcbp. We have constructed a plasmid called pET20b-fbp-rfdoc, which contains a dockerin from *R. flavefaciens*, as previously described (8). The gene of CtCBP was amplified with a pair of primers (IF-CtCBP-RfDoc and IR-CtCBP-RfDoc). The pET20b vector bone containing rfdoc was amplified with a pair of primers (VF-CtCBP-RfDoc and VR-CtCBP-RfDoc) from pET20b-fbp-rfdoc. This plasmid pET20b-ctcbp-rfdoc was constructed based on two DNA fragments by simple cloning (7).

Recombinant Protein Expression. The strains *E. coli* BL21 Star (DE3) containing the protein expression plasmids were cultivated in the LB medium supplemented with 1.2% (wt/vol) glycerol at 37 °C. When A_{600} reached about 0.75, 100 μM isopropyl-β-D-thiogalactopyranoside (final concentration) was added and the cultivation temperature was decreased to 16 °C for ∼16 h. After centrifugation, the cell pellets were resuspended in a 100 mM Hepes buffer (pH 7.5). The cells were lysed by ultrasonication. Protein purification of His-tag–containing protein was conducted routinely as published elsewhere using Ni nitrilotriacetic acid resin (1, 3, 10, 11).

Synthesis of Avicel-Containing Nanomagnetic Particles. Avicel-containing nanomagnetic particles (A-NMPs) were synthesized according to the solvothermal synthesis method (12, 13) with some modifications: 0.338 g of iron chloride ($FeCl_3O{\cdot}6H_2O$, 1.25 mmol) was completely dissolved in 10 mL of ethylene glycol to form a clear yellow solution, followed by the addition of 1.36 g of sodium acetate ($NaAc{\cdot}3H_2O$, 10 mmol) and 0.125 of Avicel. The mixture was stirred vigorously for 30 min, and the container was sealed and heated at 200 °C for 12 h. The products were cooled down at room temperature. The A-NMPs were collected by magnet to wash them with ethanol and then dried at 60 °C for 6 h.

One-Step Purification and Coimmobilization of CBP–PGP and Their Activity Assay Compared with a Mixture of CBP and PGP. After roughly estimating each targeted protein expression level by SDS/PAGE, 3 mL of cell extract of Mini-Scaf, 10 mL of cell extract of CBP-RfDoc, and 30 mL of cell extract of Ctdoc-LL-PGP were mixed with 200 mg of A-NMPs for adsorbing the CBM-containing

enzyme complex at room temperature. After centrifugation at 2,300 × *g* for 10 min, the pellets were washed in 20 mL of 100 mM Hepes (pH 7.5) containing 1 mM $CaCl_2$ three times. After centrifugation at 2,300 × *g* for 10 min, the pellets were obtained as A-NMPs immobilized enzyme complex.

Enzymatic Conversion of Cellulose. Enzymatic cellulose hydrolysis experiments were conducted in 1 mL of 50 mM Hepes buffer (pH 7.3) containing 20 g/L RAC at a rotary rate of 250 rpm at 45 °C. The enzyme loadings were 40 μg/mL each or 80 μg/mL for two-enzyme mixtures. The reactions were terminated at hour 24 by 5-min water boiling. The cellodextrin composition of enzymatic hydrolysis was measured using an HPLC equipped with a Bio-Rad HPX-42A column (1, 5).

Cellulose hydrolysis yield (X) was calculated based on the equation

$$X = \frac{G_f}{S_i} \times 100\%,$$

in which G_f was the amount of soluble sugars in the liquid phase after hydrolysis [grams per liter of glucose equivalent (GE)] and S_i was the initially added solid cellulose in terms of glucose equivalent (grams of GE per liter). The soluble sugars can be measured by using the phenol-sulfuric acid method directly (14). The cellulose amount can be measured by the modified quantitative saccharification (15).

Enzymatic Conversion of Cellulose to Amylose. Enzymatic cellulose hydrolysis experiments were conducted in 1 mL of 50 mM Hepes buffer (pH 7.3) containing 20 g/L RAC at a rotary rate of 250 rpm at 45 °C. The enzyme loadings were 40 μg/mL each for endoglucanase, cellobiohydrolase, cellobiose phosphorylase, and PGP. Maltotetraose was added as a primer for the amylose synthesis. The reactions were terminated at hour 24 by 5-min water boiling. The reactions for cellulose-to-starch experiments were terminated by 5-min water boiling. After centrifugation, which removed denatured and precipitated enzymes, the supernatants were mixed with an equal volume of 100% ethanol to precipitate the synthetic amylose. The precipitated starch amylose was washed once with ethanol followed by 6 M guanidinium chloride for eluting the residual protein from the precipitated amylose. The number of glucose units in the amylose was measured by the phenol-sulfuric acid assay (16) or enzymatic hydrolysis of glucoamylase followed by an enzymatic glucose assay kit or analysis with an HPLC equipped with a Bio-Rad HPX-42H column.

Amylose Calculations and Characterizations. Yield of amylose (Y_A) was calculated based on the equation

$$Y_A = \frac{Amylose}{S_i - S_r} \times 100\%,$$

in which *Amylose* was the amount of amylose that was separated from the hydrolysate by using ethanol precipitation (grams per liter, GE), S_i was the initially added solid cellulose in terms of GE, and S_r was the residual cellulose after enzymatic hydrolysis. The cellulose amount can be measured by modified quantitative saccharification (15).

The degree of polymerization (DP) of amylose was calculated as

$$DP = \frac{GE}{RE},$$

where *GE* is the concentration of glucose equivalents measured by the phenol-sulfuric acid method and *RE* is the concentration of reducing ends measured by the modified bicinchoninic acid method (16). Alternatively, the estimated DP of amylose was based on a ratio of glucose equivalents synthesized to maltodextrin added.

Synthetic amylose was characterized by four methods: (*i*) iodine dyeing, (*ii*) amylase hydrolysis, (*iii*) NMR, and (*iv*) FTIR. The cross-polarization magic-angle spinning ^{13}C-NMR spectra of all samples were obtained on a Bruker II Avance-300 spectrometer (17, 18). The FTIR spectroscopy was conducted using a Thermo Nicolet 6700 ATR/FT-IR spectrometer (Thermo Fisher Scientific). Two hundred fifty-six scans at a resolution of 6 cm^{-1} were averaged for each sample. All FTIR spectra were subjected to Saviszky–Golay smoothing. The absorbance of the bands obtained were resolved using Voigt distribution function by PeakFit 4.12 software.

Simultaneous Enzymatic Biotransformation and Fermentation. Simultaneous enzymatic biotransformation and fermentation (SEBF) was conducted under the following conditions: 100 mM Hepes buffer (pH 7.3) containing 20 g/L RAC, 38 g/L organic solvent-based lignocellulose fractionation-pretreated corn stover or 80 g/L diluted acid-pretreated corn stover, 0.2 mg/mL purified BsCel5, 0.1 mg/mL purified CpCel48, 0.4 mg/mL commercial TrCel7A, 0.2 mg/mL purified A-NMPs immobilized CtCBP–PGP enzyme complex, 10 mM phosphate, 75 μM maltodextrin (419699; Sigma; dextrose equivalent of 16.5–19.5 and DP of 5.8), and yeast cells (final OD 0.5). Pretreated biomass was washed with water three times before use. Yeast cells were washed three times in PBS buffer (24 g/L NaCl, 0.6 g/L KCl, 5.4 g/L $Na_2HPO_4{\cdot}2H_2O$, and 0.84 g/L KH_2PO_4) three times before mixing with other components. The reactions were carried on at 37 °C. The samples were taken at hour 12. The reactions were terminated by 5-min water boiling. After centrifugation, which removed denatured and precipitated enzymes, the supernatants were mixed with an equal volume of 100% ethanol to precipitate the synthetic starch. The precipitated starch was washed once with ethanol. The number of glucose units in the starch was measured by the phenol-sulfuric acid assay (16).

Other Assays. Protein mass concentration was measured by the Bio-Rad Bradford protein dye reagent method with BSA as a reference. The protein mass based on the Bradford method was calibrated by their absorbance (280 nm) in 6 M guanidine hydrochloride. The purity of protein samples was examined by 12% SDS/PAGE. The SDS/PAGE was stained by Bio-Rad Bio-Safe Colloidal Coomassie Blue G-250. The intensity of the band in the gel was analyzed with Quantity One (version 4.6.7; Bio-Rad).

1. Liao HH, Zhang XZ, Rollin JA, Zhang Y-HP (2011) A minimal set of bacterial cellulases for consolidated bioprocessing of lignocellulose. *Biotechnol J* 6(11):1409–1418.
2. You C, Zhang X-Z, Sathitsuksanoh N, Lynd LR, Zhang Y-HP (2012) Enhanced microbial utilization of recalcitrant cellulose by an ex vivo cellulosome-microbe complex. *Appl Environ Microbiol* 78(5):1437–1444.
3. Zhang X-Z, Sathitsuksanoh N, Zhu Z, Percival Zhang YH (2011) One-step production of lactate from cellulose as the sole carbon source without any other organic nutrient by recombinant cellulolytic Bacillus subtilis. *Metab Eng* 13(4):364–372.
4. Ye X, Zhu Z, Zhang C, Zhang Y-HP (2011) Fusion of a family 9 cellulose-binding module improves catalytic potential of *Clostridium thermocellum* cellodextrin phosphorylase on insoluble cellulose. *Appl Microbiol Biotechnol* 92(3):551–560.
5. Zhang Y-HP, Lynd LR (2003) Cellodextrin preparation by mixed-acid hydrolysis and chromatographic separation. *Anal Biochem* 322(2):225–232.
6. Zhu Z, et al. (2009) Comparative study of corn stover pretreated by dilute acid and cellulose solvent-based lignocellulose fractionation: Enzymatic hydrolysis, supramolecular structure, and substrate accessibility. *Biotechnol Bioeng* 103(4):715–724.
7. You C, Zhang X-Z, Zhang Y-HP (2012) Simple cloning via direct transformation of PCR product (DNA Multimer) to *Escherichia coli* and *Bacillus subtilis*. *Appl Environ Microbiol* 78(5):1593–1595.
8. You C, Myung S, Zhang Y-HP (2012) Facilitated substrate channeling in a self-assembled trifunctional enzyme complex. *Angew Chem Int Ed Engl* 51(35): 8787–8790.

9. You C, Zhang X-Z, Zhang YHP (2012) Mini-scaffoldin enhanced mini-cellulosome hydrolysis performance on low-accessibility cellulose (Avicel) more than on high-accessibility amorphous cellulose. *Biochem Eng J* 63:57–65.
10. Zhang X-Z, Zhang Y-HP (2011) Simple, fast and high-efficiency transformation system for directed evolution of cellulase in *Bacillus subtilis*. *Microb Biotechnol* 4(1):98–105.
11. Wang Y, Huang W, Sathitsuksanoh N, Zhu Z, Zhang Y-HP (2011) Biohydrogenation from biomass sugar mediated by *in vitro* synthetic enzymatic pathways. *Chem Biol* 18(3):372–380.
12. Deng H, et al. (2005) Monodisperse magnetic single-crystal ferrite microspheres. *Angew Chem Int Ed Engl* 117(18):2842–2845.
13. Huang X, et al. (2009) General strategy for designing functionalized magnetic microspheres for different bioapplications. *Langmuir* 25(19):11657–11663.
14. Zhang Y-HP, Cui J, Lynd LR, Kuang LR (2006) A transition from cellulose swelling to cellulose dissolution by o-phosphoric acid: Evidence from enzymatic hydrolysis and supramolecular structure. *Biomacromolecules* 7(2):644–648.
15. Moxley G, Zhang Y-HP (2007) More accurate determination of acid-labile carbohydrate composition in lignocellulose by modified quantitative saccharification. *Energy Fuels* 21:3684–3688.
16. Zhang Y-HP, Lynd LR (2005) Determination of the number-average degree of polymerization of cellodextrins and cellulose with application to enzymatic hydrolysis. *Biomacromolecules* 6(3):1510–1515.
17. Bennett A, Rienstra C, Auger M, Lakshmi K, Griffin R (1995) Heteronuclear decoupling in rotating solids. *J Chem Phys* 103:6951–6958.
18. Sathitsuksanoh N, Zhu ZG, Wi S, Zhang Y-HP (2011) Cellulose solvent-based biomass pretreatment breaks highly ordered hydrogen bonds in cellulose fibers of switchgrass. *Biotechnol Bioeng* 108(3):521–529.
19. Ye X, Rollin J, Zhang Y-HP (2010) Thermophilic α-glucan phosphorylase from *Clostridium thermocellum*: Cloning, characterization and enhanced thermostability. *J Mol Catal, B Enzym* 65:110–116.

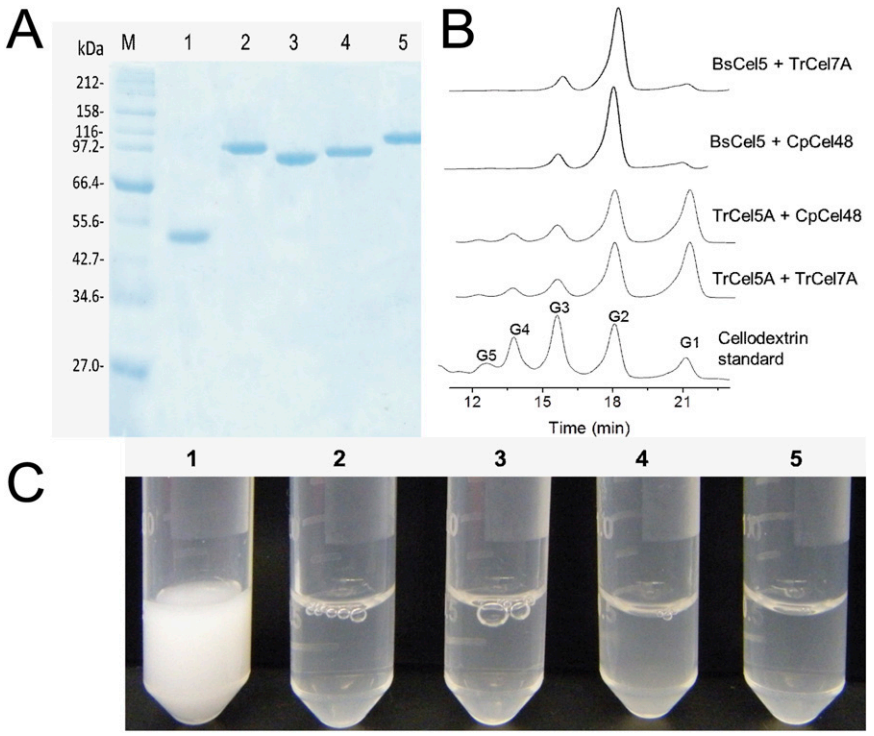

Fig. S1. SDS/PAGE analysis of five purified recombinant enzymes (1, BsCel5; 2, CpCel9; 3, CpCel48; 4, CBP; and 5, PGP) produced by *E. coli* BL21 (DE3) (*A*), HPLC spectra of the two-cellulase mixture for a maximal release of cellobiose compared with glucose and cellodextrin standards (*B*), and photos of the cellulose slurry and enzymatic hydrolysate (*C*). Tube 1, 5 g/L RAC slurry; tube 2, hydrolysate generated by a mixture of BsCel5 and TrCel7A; tube 3, hydrolysate generated by a mixture of BsCel5 and CpCel48; tube 4, hydrolysate generated by a mixture of TrCel5A and CpCel48; and tube 5, hydrolysate generated by a mixture of TrCel5A and TrCel7A. The quantitative data for cellulose digestibility and cellodextrin distribution are presented in Tables S1 and S2, respectively.

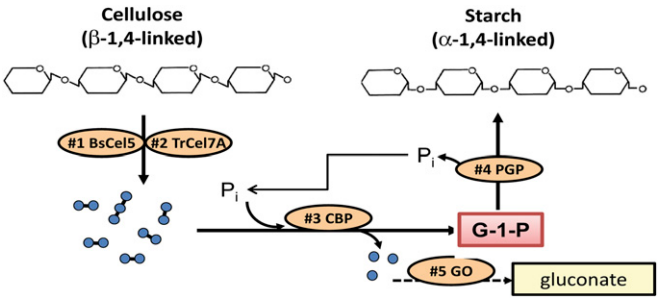

Fig. S2. Enhanced starch yields by removal of glucose, an inhibitor of CBP, by addition of glucose oxidase (GO).

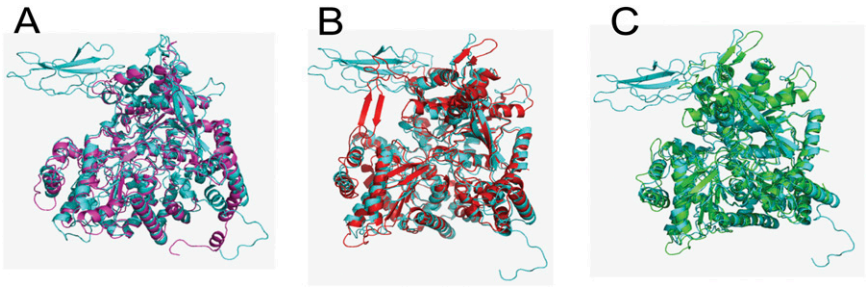

Fig. S3. Homology structure comparison between WT PGP (cyan, *A*) and the bacterial alpha-glucan phosphorylase from *Thermotoga maritime* (purple, *A*) and partially decapped PDC-PGP (red, *B*) and completely decapped CDC-PGP (green, *C*), respectively.

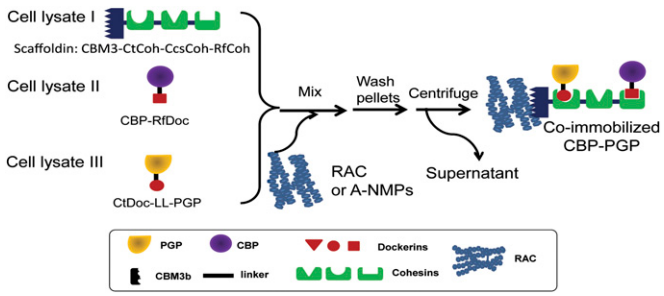

Fig. S4. One-step purification and coimmobilization of CBP-RfDoc and CtDoc-LL-PGP on the surface of regenerated amorphous cellulose (RAC) or Avicel-containing nanomagnetic particles (A-NMPs) through a synthetic CBM-containing scaffoldin.

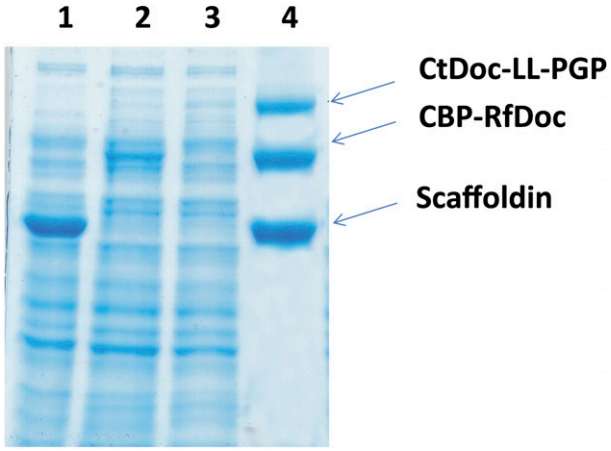

Fig. S5. SDS/PAGE analysis of the coimmobilized CBP–PGP. Lane 1, cell extract I containing scaffoldin; lane 2, cell extract II containing CBP-RfDoc; lane 3, cell extract III containing CtDoc-LL-PGP; and lane 4, RAC bound Coh3, CBP-RFDoc- and CtDoc-LL-PGP.

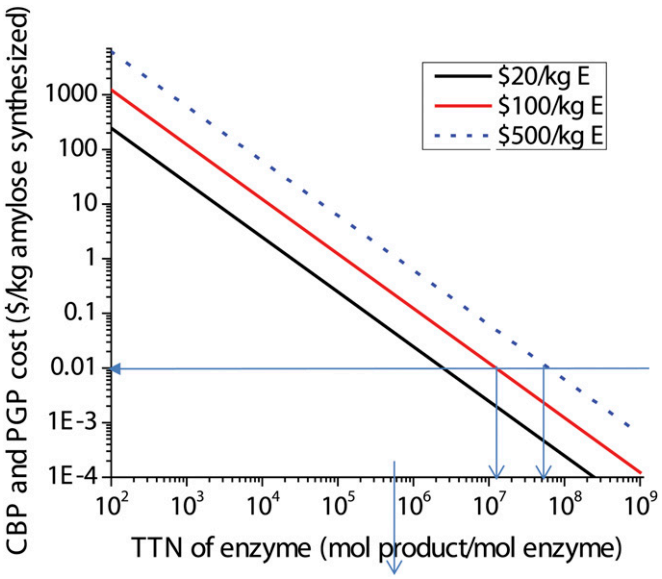

Fig. S6. Enzyme cost analysis of CBP and PGP used for the synthetic starch production as a function of total turnover number (TTN) of CBP and PGP, where an average molecular weight of CBP and PGP is 100,000. Industrial enzyme costs are assumed to be $20, $100, or $500 per kilogram of enzyme.

Table S1. Digestibility of RAC hydrolysis by individual cellulases or their cellulase mixtures

Enzyme name	Type	Cellulose degraded,* %
BsCel5	Endo	76
TrCel5A	Endo	72
CpCel9	Endo	23
TrCel7A	Exo	14
CpCel48	Exo	8.7
BsCel5/TrCel7A	Endo/exo	100
BsCel5/CpCel48	Endo/exo	98
TrCel5A/CpCel48	Endo/exo	92
TrCel5A/TrCel7A	Endo/exo	95

Enzymatic cellulose hydrolysis experiments were conducted in 50 mM Hepes buffer (pH 7.3) containing 20 g/L regenerated amorphous cellulose at 45 °C. The enzyme loading was 40 μg/mL each or 80 μg/mL for two-enzyme mixtures. The reactions were terminated after 24 h by water boiling. *The reported values are the averages of three measurements for which the SDs were less than 5%.

Table S2. Different hydrolytic product distribution of the hydrolysate by the enzyme mixtures

	Percentage,* % (wt/wt)		
Enzyme	Glucose	Cellobiose	Cellotriose
BsCel5/TrCel7A	14.1	74.3	10.5
BsCel5/CpCel48	14.0	72.4	11.3
TrCel5A/CpCel48	54.0	21.9	7.4
TrCel5A/TrCel7A	57.7	22.1	6.4

*The remaining components are small amounts of G4-G6. Reported values are the averages of three measurements for which the SDs were less than 2%.

Table S3. Yields and degree of polymerization of synthetic amylose made from cellulose

GO	Maltotetraose, μM	Amylose produced, g/L	Degree of polymerization		Amylose yield, % (wt/wt)
			Measured	Estimated	
–	50	2.10	210	249	10.5
–	75	2.28	168	188	11.4
–	100	3.14	161	193	15.7
–	125	2.88	142	160	14.4
+	100	6.00	246	370	30.0

Cellulose-to-starch experiments were conducted in a mixed buffer: 50 mM Hepes buffer (pH 7.3) and 30 mM sodium phosphate salt (pH 7.0) containing 20 g/L RAC and 50–125 μM maltoteraose at 45 °C. The enzyme loadings were 40 μg/mL BsCel5, 40 μg/mL TrCel11, 40 μg/mL CBP, and 40 μg/mL PGP for all cases. Glucose oxidase (GO) was added if necessary (3 mg/mL). –, no GO added; +,GO added. The reactions were terminated after 24 h by 5-min water boiling. All RACs were hydrolyzed under these conditions. Reported values are the averages of three measurements and their SDs were less than 5%. The whole cellulose-to-amylose pathway is shown in Fig. S2.

Table S4. Primer sequences used in this study

Primer	Sequence
VF-Scaf	TACTGATGGCGCTATCATTGTTAAGCTCGAGCACCACCACCACCACCACT
VR-Scaf	CCTTCAAATTGCCTGATACCGGCATATGTATATCTCCTTCTTAAAGTTAA
IF-Scaf	TTAACTTTAAGAAGGAGATATACATATGCCGGTATCAGGCAATTTGAAGG
IR-Scaf	AGTGGTGGTGGTGGTGGTGCTCGAGCTTAACAATGATAGCGCCATCAGTA
IF-CtDoc	ACTTTAAGAAGGAGATATACATATGGGCGACGTCAATGATGACGGAAAAG
VR-CtDoc	CTTTTCCGTCATCATTGACGTCGCCCATATGTATATCTCCTTCTTAAAGT
VF-LL-PGP	ACCGCCGTCAGATGATCCGAATGCAGCGACTGCGAATGGAGCACACCTGT
IR-LL-PGP	ACAGGTGTGCTCCATTCGCAGTCGCTGCATTCGGATCATCTGACGGCGGT
IF-LL-PGP	AATAGATACATTGCCGTACAAGAACTTTACAGGCGGAACTCTTGAACCGG
VR-LL-PGP	CCGGTTCAAGAGTTCCGCCTGTAAAGTTCTTGTACGGCAATGTATCTATT
IF-PGP	ACTTTAAGAAGGAGATATACATATGGCGACTGCGAATGGAGCACACCTGT
VR-PGP	ACAGGTGTGCTCCATTCGCAGTCGCCATATGTATATCTCCTTCTTAAAGT
VF- PGP	GAACATTGAAGCAGTTGAAATCGCA TGAGATCCGGCTGCTAACAAAGCCC
IR- PGP	GGGCTTTGTTAGCAGCCGGATCTCATGCGATTTCAACTGCTTCAATGTTC
PGP_CDC-F	CCGCCGAAAAAAGTGCGCATGGCCAATC
PGP_CDC-R	GTTTTCCAGAATACGCATAGTCGTCAG
PGP_PDC-F	AAGAAAACCCCGGTCAGCCCGGAAC
PGP_PDC-R	TTCCGGTTTAATGAACAGTTCCGCG
IF-CBP-RfDoc	TTAACTTTAAGAAGGAGATATACATATGAAGTTCGGTTTTTTTGATGATG
VR-CBP-RfDoc	CATCATCAAAAAAACCGAACTTCATATGTATATCTCCTTCTTAAAGTTAA
VF-CBP-RfDoc	CACAAAGTTGAAGTAATTATGGGACCCGGCACAAAGCTCGTTCC
IR-CBP-RFDoc	GGAACGAGCTTTGTGCCGGGTCCCATAATTACTTCAACTTTGTG

Table S5. Strains and plasmids used in this study

Strains or plasmids Strains	Characteristics	Source
E. coli Top10	*F- mcrA Δ(mrr-hsdRMS-mcrBC) φ80lacZΔM15 ΔlacX74 nupG recA1 araD139 Δ(ara-leu)7697 galE15 galK16 rpsL(StrR) endA1 λ-*	Invitrogen
E. coli BL21 Star (DE3)	F⁻*ompT hsd*SB (rB⁻mB⁻) *gal dcm rne131* (DE3)	Invitrogen
Saccharomyces cerevisiae S288c	*MATα SUC2 gal2 mal mel flo1 flo8-1 hap1*	Gift from Hong Lv (Fudan University, Shanghai, China)
Plasmids		
pET20b-miniscaf	Amp^R, with miniscaffoldin expression cassette cloned, containing a CBM module from *C. thermocellum* and three different cohesins from *C. thermocellum*, *C. cellulovorans*, and *R. flavefaciens,* respectively.	(1)
pET20b-pgp	Amp^R, with pgp expression cassette cloned. PGP module was from *Solanum tuberosum* This enzyme was purified based on the c-terminal 6X His tag.	This work
pET20b-ctdoc-ll-pgp	Amp^R, with ctdoc-ll-pgp expression cassette cloned, PGP module was from *Solanum tuberosum,* the dockerin module was from *C. thermocellum* Cel48. Long linker module was from *C. thermocellum* CipA.	This work
pET20b-ctdoc-ll-pdc-pgp	Amp^R, with ctdoc-ll-pgp expression cassette cloned, pdc-PGP module was derived from PGP of partially decapped. The dockerin module was from *C. thermocellum* Cel48. Long linker module was from *C. thermocellum* CipA.	This work
pET20b-ctdoc-ll-cdc-pgp	Amp^R, with ctdoc-ll-pgp expression cassette cloned, pdc-PGP module was derived from PGP of completely decapped. The dockerin module was from *C. thermocellum* Cel48. Long linker module was from *C. thermocellum* CipA.	This work
pET20a-ctcbp	Amp^R, with ctcbp-rfdoc expression cassette cloned, CtCBP module was from *C. thermocellum.* This enzyme was purified based on the C-terminal 6X His tag.	(2)
pET20a-ctcbp-rfdoc	Amp^R, with ctcbp-rfdoc expression cassette cloned, CtCBP module was from *C. thermocellum.* The dockerin was from *R. flavefaciens.*	This work
pET20a-bscel5	Amp^R, with BsCel5 expression cassette cloned, Cel5 was from *Bacillus subtilis* 168. This enzyme was purified based on the C-terminal 6X His tag.	(3)
pET20b-cpcel9	Amp^R, with CpCel9 expression cassette cloned.Cel9 was from *Clostridium phytofermentans*. This enzyme was purified based on the C-terminal 6X His tag.	(3)
pET20a-cpcel48	Amp^R, with CpCel48 expression cassette cloned.Cel48 was from *Clostridium phytofermentans*. This enzyme was purified based on the C-terminal 6X His tag.	(3)

1. You C, Myung S, Zhang Y-HP (2012) Facilitated substrate channeling in a self-assembled trifunctional enzyme complex. *Angew Chem Int Ed Engl* 51(35):8787–8790.
2. Ye X, Rollin J, Zhang Y-HP (2010) Thermophilic α-glucan phosphorylase from *Clostridium thermocellum*: Cloning, characterization and enhanced thermostability. *J Mol Catal, B Enzym* 65:110–116.
3. Liao HH, Zhang XZ, Rollin JA, Zhang Y-HP (2011) A minimal set of bacterial cellulases for consolidated bioprocessing of lignocellulose. *Biotechnol J* 6(11):1409–1418.